Ocean Science Journal, *Vol. 40, No. 2, 101-107(2005)*

Note

Ocean Science Journal

http://library.kordi.re.kr/OceanScience/

Abyssal Currents Driven by a Local Wind Forcing through Deep Mixed Layer: Implication to the East Sea

Young Ho Seung

Department of Oceanography, College of Natural Science, Inha University, Incheon 402-751, Korea

Received 3 January 2005; Revised 23 May 2005; Accepted 30 May 2005

Abstract – A simple analytical model is considered in an attempt to demonstrate a formation mechanism of the abyssal current in the East Sea. In this model, the abyssal currents are driven by wind through an outcrop region and flow along closed geostrophic contours. A rough estimate of the abyssal currents, arrived at by applying this model to the region of deep mixing in the East Sea, gives currents comparable to those observed, although there is an uncertainty in the surface area of the outcrop region. It seems that the spin-up of deep water by wind forcing through the region of deep winter mixing is, at least partly, an important contribution to the formation of the abyssal currents in the East Sea.

Key words – Abyssal current, East Sea, deep mixed layer

1. Introduction

The Tsushima Current, a warm current originating from Kuroshio, enters the East Sea through the Korea/Tsushima Strait. It extends up to about 38-40^0 N north, where cold surface water is found. A subpolar front exists between the southern warm and northern cold waters. North of the subpolar front, a current called the North Korea Cold Current (NKCC) or the Liman Current (LC) flows southward along the North Korean and Siberian coasts. It then forms a cyclonic gyre north of the subpolar front (Senjyu and Sudo 1994; Isobe and Isoda 1997). The NKCC/LC is known to be driven by the wind with positive stress curl and surface cooling (Seung 1992).

North of the subpolar front, the surface current extends downward to a considerable depth, such that the surface and intermediate circulations are not distinguishable from each other. This current overlies a deep homogeneous layer extending down to the bottom: The intermediate and deep waters are formed by deep winter mixing off the northwestern coastal area (Seung and Yoon 1995; Kawamura and Wu 1998). This deep surface current in the north extends southward across the subpolar front, supplying the fresh and high-oxygen content intermediate water, the so-called East Sea Intermediate Water (Kim and Chung 1982), below the Tsushima Current Water. The formation of the intermediate circulation beneath the Tsushima Current can be explained by the ventilation theory (Luyten *et al.* 1983), as demonstrated analytically by Seung (1997) and modeled numerically by Kim and Seung (1999) and by Yoon and Kawamura (2002). According to this theory, the intermediate layer is forced by the wind over the outcrop region north of the subpolar front. It then forms a cyclonic gyre, conserving the potential vorticity. How far southward it penetrates from the subpolar front depends on the magnitude of wind stress curl. The explanation given above assumes that the intermediate layer overlies a motionless deep lower layer. In reality, however, the lower layer moves relatively fast above the bottom. In this respect, the dynamics of the intermediate circulation explained by the ventilation theory needs to be modified.

In the deep homogeneous layer underlying the intermediate layer, strong abyssal currents are observed. They are mostly oscillatory, probably associated with eddy-like features, with current magnitude occasionally reaching up to 10 cm/sec (Takematsu *et al.* 1999; Senjyu *et al.* 2002). However, the mean current is generally of the order of 1 cm/sec, and seems to run cyclonically along the steep bottom slope (Chang *et al.* 2002). Senjyu *et al.* (2002) observed especially strong abyssal currents, also mostly oscillatory, which lasted for a relatively long time after the event of deep water formation. They conjecture that the former is spun up by the latter.

Some numerical models succeeded in reproducing the abyssal currents, thanks either to hypothesizing the eddy-topography interaction, the so-called neptune effect (Holloway

*Corresponding author. E-mail: seung@inha.ac.kr

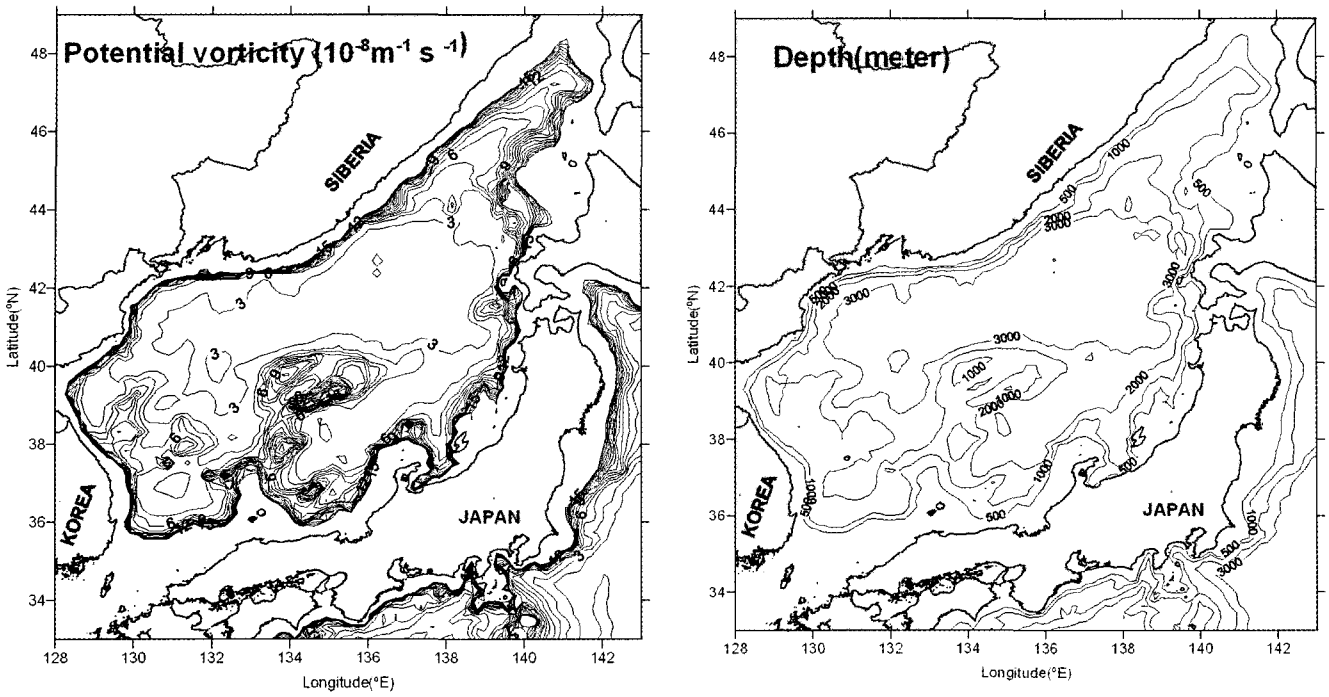

Fig. 1. Geostrophic contours (contours of potential vorticity f/H with f, Coriolis parameter and H, bottom depth) and bottom topography of the East Sea.

et al. 1995), or to very fine horizontal grid resolution (Hogan and Hulbert 2000; HH hereafter). In HH, they argue that the obtained realistic abyssal currents may be due to the baroclinic instability. Recently, Yoon (private communication) developed a numerical model with horizontal resolution comparable to, but vertically more refined than, that by HH. In this model, however, the abyssal currents appear weaker than those observed in contrast to what had been obtained in the previous models. This fact renders the role of either the neptune effect or baroclinic instability more doubtful.

The fact that the abyssal currents flow along the steep slope of the bottom is physically significant. In this basin, the bottom slope is so steep that the isobaths nearly coincide with the geostrophic contours f/H where f is the Coriolis parameter and H is bottom depth (Fig. 1). As a consequence, most geostrophic contours are closed on themselves without touching land boundaries. In fact, the theory presented by Rhines and Young (1982), which predict that even a weak forcing can generate strong abyssal currents over the closed geostrophic contours, may also be applied to the East Sea. This forcing might be the wind stress exerted on the outcropped portions of deep layer, which seem to be present in the northern part of the basin, as indicated by observations (Fig. 2). In the region of deep mixing, density stratification is so weak that the whole layer can be considered to be almost one single homogeneous layer. Hence, there emerges a need to demonstrate more rigorously the generation of the abyssal circulation by the mechanism proposed above. For this purpose, a simple analytical model is considered and then a rough estimation of abyssal currents is attempted for the East Sea. In comparison, the possibility of buoyancy-driven abyssal circulation, suggested by Senjyu *et al.* (2004), is also discussed.

2. Model

In order to demonstrate that even a weak forcing can indeed drive a significant deep current over a closed geostrophic contour in a relatively small basin with large depth change, like the East Sea, consider theoretically a two-layer circular basin with radius L and maximum depth H_0 at the center (Fig. 3). Take a right-handed cartesian coordinate with x- and y-axes pointing respectively eastward and northward, and a polar coordinate with r and θ denoting, respectively, the radial distance from the center and azimuthal angle measured anti-clockwisely from the y-axis. This basin has a uniform bottom slope H_0/L, i.e., the bottom depth H is given by $H=H_0(1-r/L)$. The basin is under a steady wind forcing which creates a basin-scale motion. The upper layer motion may also be driven by other forcing such as the inflow-outflow, like the Tsushima Current in the East Sea.

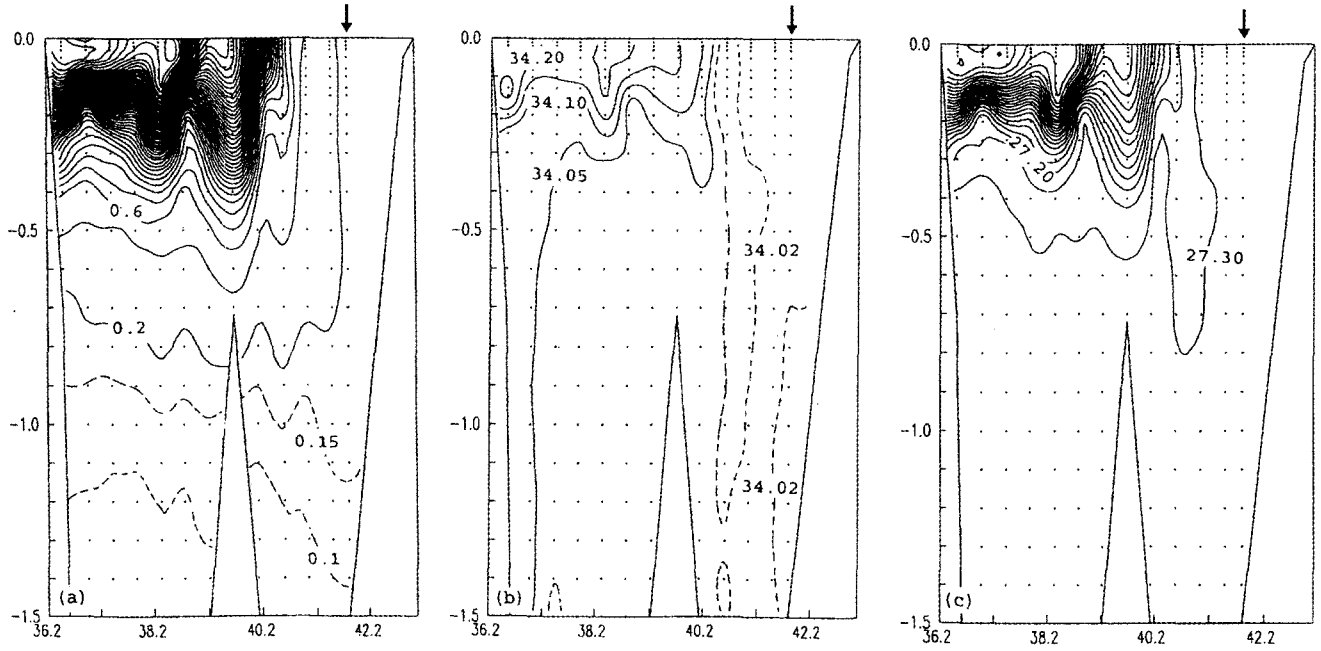

Fig. 2. Distributions of (a), potential temperature (in °C) referred to the surface; (b), salinity (in psu); and (c) potential density (in sigma unit) referred to the surface along the section located between (132.5 °E, 42.5 °N) and (136.0 °E, 36.2 °N). Abscisa is latitude calculated in degrees and the ordinate is the depth in Km. Arrows indicate deep convective mixing. See Seung and Yoon (1995) for more details.

Suppose that an outcropping of the lower layer occurs in the northern part of the basin, mimicking the deep winter mixing occurring in the East Sea. This phenomenon occurs in a narrow coastal band delineated by L-W<r<L and $-\alpha/2<\theta<\alpha/2$ (Fig. 3), where W is much smaller than L. Along the edge of the outcrop region, large changes of upper layer thickness take place on a scale comparable to the internal Rossby radius, much smaller than the basin scale L. Hence, for the problem resulting from length scale L, like the one considered here, a step-like variation of h_1 can be assumed across the edge of the outcrop. This type of approach was originally attempted by Hendershott (1989) in a problem related to ventilated thermocline. In the basin interior, away from the outcrop region, the upper layer thickness h_1 is expressed by $h_1=H_1+\eta$ where H_1 is the spatially-averaged value of h_1 and η is the deviation from the average. It is assumed that the magnitude of η is only a negligible fraction of H_1 in this region. As will become clear shortly, this means that the coupling between the upper and lower layers through pressure perturbation is very weak on the basin-scale. Applicability of this assumption to the East Sea will be discussed in the next section. With this configuration, the lower layer thickness h is given as follows:

$$h=\begin{cases} H & \text{for } L-W<r<L,\ -\alpha/2<\theta<\alpha/2 \\ \max[0,H-H_1] & \text{otherwise} \end{cases} \tag{1}$$

where η is ignored compared to H_1, as mentioned above, and H is given earlier. Note that on the offshore side of the outcrop boundary (r=L-W, $-\alpha/2<\theta<\alpha/2$), the upper layer thickness, H_1, is smaller than the bottom depth, $H=H_0W/L$, which seems to be the case for the East Sea as indicated in Figure 2. This implies that

$$W>H_1L/H_0 \tag{2}$$

The right-hand side of (2) is very small compared to L because H_1/H_0 is much smaller than unity.

The potential vorticity conservation for the lower layer is governed by

$$h\vec{V}\cdot\nabla q=\vec{k}\cdot\nabla\times[(\vec{\tau}/\rho-\mu\vec{V})/h] \tag{3}$$

where $\vec{V}$ is the lower layer current vector, $\vec{k}$ is the unit vector in an upward direction, $\vec{\tau}$ is the wind stress vector acting on the outcropped lower layer surface, ρ is the density, and μ is the linear bottom friction coefficient. The potential vorticity q is given by

$$q=(f+\zeta)/h=(f_0/h)(1+\beta y/f_0+\zeta/f_0)\simeq f_0/h \tag{4}$$

where $f=f_0+\beta y$, the Coriolis parameter, increases meridionally with the coefficient of planetary effect β and ζ is the relative vorticity. In (4), magnitudes of the planetary effect and that of the relative vorticity compared to f_0/h

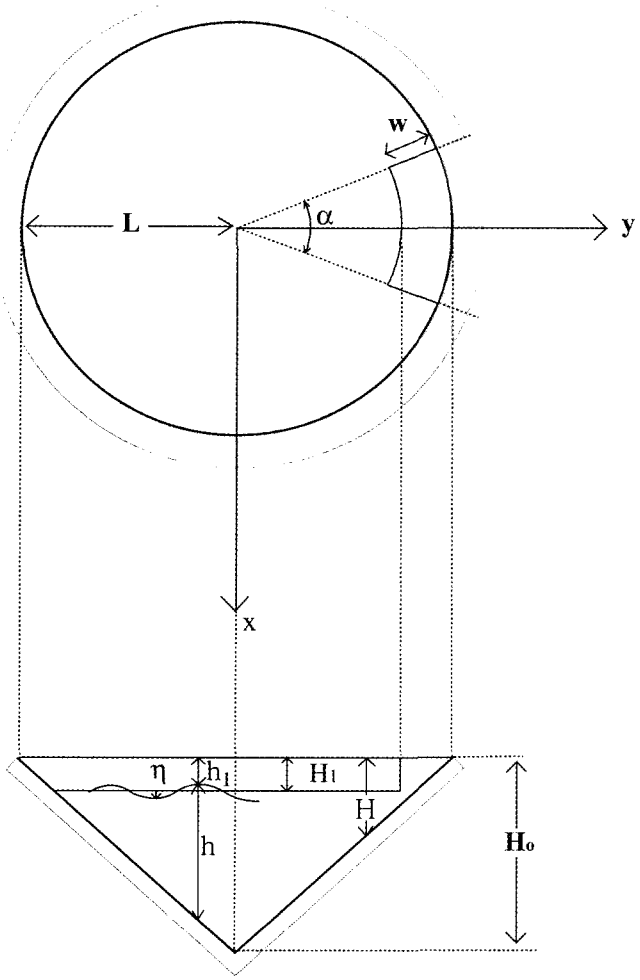

Fig. 3. Plan and side views of the circular basin with bottom depth H linearly increasing to H_0 at the center. The lower layer (thickness h) outcrops to the surface in the coastal band of width W and azimuthal angle α (shaded). The upper layer thickness, h_1, consists of mean H_1 and deviation from the mean, η.

are, respectively, of the order $\beta L/f_0$ and U/f_0L (Rossby number with U velocity scale). For weak motions in a relatively small basin with a steep bottom slope, these can be considered negligibly small, as shown in the next section. Since the relative magnitude of change of h over the length scale L, $\Delta h/h$, is of the order of unity, change of q, Δq, can also be approximated by $\Delta(f_0/h)$, as can be deduced from (4). Hence, the potential vorticity contours (or geostrophic contours) approximately coincide with those of h. Equation (3) is the same as that considered by Rhines and Young (1982) in their theory of planetary geostrophic circulation over a closed geostrophic contour.

Consider a closed contour of q, say Γ, passing through the outcrop region (Fig. 4). This contour consists of two circular arcs, one outside the outcrop region with radius R

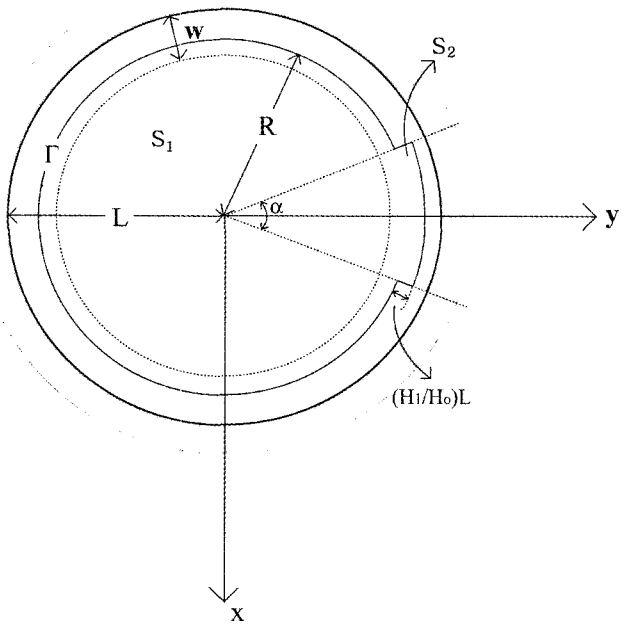

Fig. 4. Closed geostrophic contour Γ (solid line) passing through the outcrop region. It consists of a circular arc of radius R outside the outcrop region and a circular arc of radius $R+H_1L/H_0$ inside the outcrop region. The region enclosed by Γ consists of the subregion S_1 shielded from the wind and the subregion S_2 exposed to the wind (shaded).

and the other in the outcrop region with radius $R+H_1L/H_0$, and two lines connecting these two circular arcs. One comment may be necessary about the latter fact. There is a discontinuity in q across the segment $R<r<R+H_1L/H_0$ between these two circular arcs. However, this discontinuity certainly includes the value of q defined along Γ. For later convenience, the whole region enclosed by Γ is referred to as S, the subregion within S shielded from the wind as S_1, and the other subregion under direct wind forcing as S_2, such that the region S consists of S_1 and S_2. In the region S_1, the wind forcing in the right-hand side of (3) vanishes. The frictional effect in the right-hand side of (3) is of order $\mu U/LH_0$. The advection terms on the left-hand side are of the order f_0U/L. Hence, the former is of the order μ/f_0H_0 (<<1) compared to the latter, which is the ratio of frictional decay time to inertial period. Hence, in region S_1, (3) is approximated as

$$h\vec{V}\cdot\nabla q = 0 \tag{5}$$

Equation (5) indicates that in region S_1, current is mostly along-slope, which is yet to be sought. In region S_2, the ratio of bottom frictional force to wind stress force, both on the right-hand side of (3), is $C_DU^2/(\tau/\rho)$ when use is made of $\mu=C_D|\vec{V}|$. For typical values of $|\vec{\tau}|/\rho=10^{-4}$ m^2/sec^2,

$C_D=2\times10^{-3}$, and for U of the order 10^{-2} m/sec, this is much smaller than unity. Hence, (3) can be approximated as

$$h\vec{V}\cdot\nabla q=\vec{k}\cdot\nabla\times(\vec{\tau}/\rho h) \tag{6}$$

The solution to (6) consists of two modes. One is the free mode corresponding to the general solution to (6), which has the same form as that obtained from (5). The other is the forced mode induced by the wind stress curl. The free mode current is along-slope and is connected to the same free mode current in region S_1. Hence, it can be assumed that the along-slope (free mode) current in region S_2 has the same order of magnitude as that in region S_1. The forced mode current is cross-slope and its magnitude is proportional to the strength of wind stress curl. This cross-slope transport is compensated for by that found in region S_1, so that the net transport across Γ vanishes. In fact, Rhines and Young (1982) have already found that the circulation over a closed geostrophic contour is dominated by the free mode.

In order to seek the abyssal current, mostly along-slope, integrate (3) over the region S. The left-hand side of (3) identically vanishes, which can be easily shown by using the continuity, $\nabla\cdot h\vec{V}=0$, divergence theorem, and reminding that q=const. along Γ:

$$\iint_S h\vec{V}\cdot\nabla q\,ds=\iint_S(\nabla\cdot h\vec{V}q-q\nabla\cdot h\vec{V})ds=$$

$$q\oint_\Gamma hV_n\,dl=0 \tag{7}$$

where s denotes the surface area in region S, l is the length along Γ and V_n is the component of $\vec{V}$ outward normal to Γ. In (7), the line integration is in a counter-clockwise direction. Area integration of the right-hand side of (3) can be done using the stokes theorem. In doing so, $\mu=C_D|\vec{V}|=C_DV_l$ is applied, where V_l is the tangential component of $\vec{V}$ to Γ in a counter-clockwise direction. Note that $\vec{V}$ is largely along-slope, and its direction is counter-clockwise for positive wind stress curl. (It is seen shortly that the mean wind stress curl is positive in the East Sea.) The result is

$$\iint_{S_2}T/h\,ds+\iint_{S_2}\vec{k}[\nabla(1/h)\times\vec{\tau}/\rho]ds-\frac{C_D}{h(R)}\oint_\Gamma V_l^2dl=0 \tag{8}$$

where $T=\vec{k}\cdot\nabla\times(\vec{\tau}/\rho)$ and h(R) is h at r=R, constant along Γ.

3. Application to the East Sea

In the East Sea, the volume transport in the upper layer, relative to the lower layer, is usually considered to be about 2 Sverdrups across the basin. Thus, from the thermal wind relationship, it can be said that

$$g'\Delta(h_1^2)/(2f)\sim H_1g'\eta/f_0=2\text{ Sverdrups} \tag{9}$$

where $\Delta(h_1^2)$ the basin-wide change of h_1^2 and g' is the reduced gravity. Taking $g'=2\times10^{-2}$ m/sec^2, $f_0=10^{-4}$ sec^{-1} and $H_1=3\times10^2$ m, the magnitude of η is about 30 m which is sufficiently smaller than H_1 for η to be neglected compared to H_1, especially so in the model where the orders of magnitude of physical quantities are sought. The length scale of the basin L is of the order 10^6 m. The Rossby radius, given by $\sqrt{g'H_1}/f_0$, is a few tens of kilometers, much smaller than L, justifying the assumption of step-like variation of h_1 near the outcrop boundary. Taking the value β, to be 2×10^{-11} m^{-1}sec^{-1}, $\beta L/f_0$ is about 0.2, marginally satisfying the condition taken in (4). Finally, the Rossby number, $\zeta/f_0=U/Lf_0$, is of the order of 10^{-2} for velocity scale U of order 1 cm/sec, also satisfying the condition in (4).

Na *et al.* (1992) estimated wind stresses from climatological atmospheric pressure distribution. According to them, wind is relatively strong in winter especially in the northwestern part of the basin, where deep winter mixing is observed (Seung and Yoon 1995). Annual mean wind stress curl in this region is of the order of 10^{-7} N/m^2 which, in (8), gives $T=10^{-10}$ m/sec^2. Wind stress is largely perpendicular to isobathic lines and we neglect the second term on the left-hand side of (8). For reference, the January monthly mean wind stress from NSCAT observations in 1997 (Kawamura and Wu 1998) was about 1.8 dyn/cm^2, much larger than the winter-mean value, 1.0 dyn/cm^2, obtained by Na *et al.* (1992). Assuming that T is uniform over the outcrop region, (8) becomes, to order H_1/H_0,

$$\frac{\alpha TL^2}{H_0}[ln(1/\delta)-W(1-\delta)/L]=2\pi RC_D\bar{L}\bar{V}_l^2/\delta H_0W \tag{10}$$

where $\delta=(L-R)/W(<1.0)$ and the over bar denotes average over Γ. If we take Γ such that it passes the outcrop region sufficiently far from the offshore edge, δ becomes sufficiently smaller than 1.0 for the second term in (10) to be neglected compared to the first term. The result is

$$\bar{V}_l^2=\frac{\alpha TWL}{2\pi C_DR}\delta ln(1/\delta)\simeq\frac{TL\lambda}{2C_D}\delta ln(1/\delta) \tag{11}$$

where $\lambda=\alpha WL/\pi LR$ is approximately the ratio of the area of outcrop region to that of the whole basin, as shown subsequently. The area of the outcrop region, say A, is given by

$$A=\frac{\alpha}{2}[L^2-(L-W)^2]=\alpha WL(1-W/2L)\simeq\alpha WL \tag{12}$$

to the order W/2L. For the surface area of the basin, the relationship

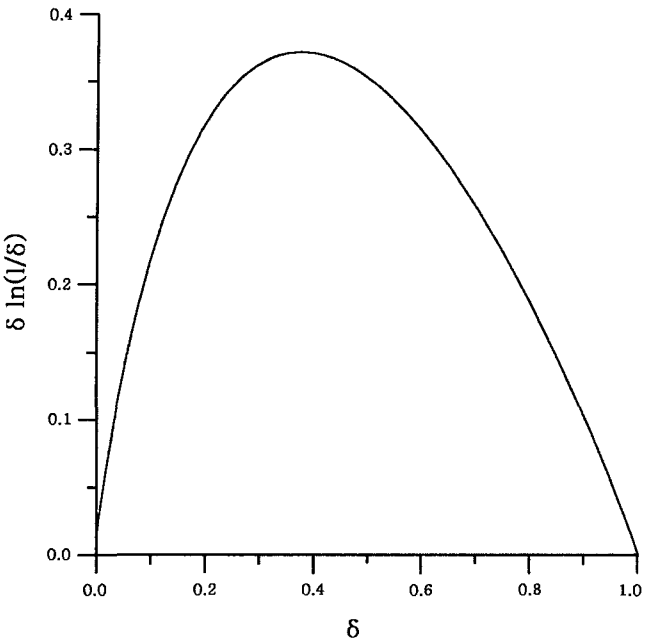

Fig. 5. Values of $\delta \ln(1/\delta)$ as a function of δ.

$$\pi LR = \pi L^2(1-\delta W/L) \simeq \pi L^2 \quad (13)$$

holds to order $\delta W/L$. The values of $\delta \ln(1/\delta)$ in (11) range from 0 to about 0.35 for $0<\delta<1$(Fig. 5). Hence, for moderate δ, they are of the order 10^{-1}.

The greatest uncertainty lies in λ. Up till now, there is no available observation indicating surface area of the outcrop, although the outcrop is known to present. Numerical experiments (Kim and Seung 1999; Yoon and Kawamura 2002) show that vertical convection reaching down to a depth of 1000 m takes place over the area with a length scale of about 100 km to the north of the basin in the winter season. Below the deep mixed layer in the convection region, density stratification is usually very weak with the relative density difference between the mixed layer and the bottom layer being less than 10^{-5} (see Fig. 7 in Yoon and Kawamura 2002 for example). Considering this fact, we think that λ in (11) would be of the order of 10^{-2}. Using the parameter values given above, (11) gives V_I of the order of 1 cm/sec, which is the same as the magnitude of the observed mean currents (~1 cm/sec).

4. Conclusions and Discussion

As mentioned above, the results are highly dependent on the surface area of the outcrop region, which is not accurately known. Suppose that $\lambda=10^{-3}$ in (11) is the lowest possible limit. For this value of λ, V_I becomes about 0.3 cm/sec, which is still an important contribution to the observed mean abyssal current (~1 cm/sec). Hence, we conclude that the abyssal current in the East Sea might indeed be driven, at least partly, by a local wind forcing through deep convective mixing present in the northwestern part of the basin in winter. The internal stress exerted by the upper moving layers, such as the intermediate layer, may also add to driving the abyssal current. As suggested by Senjyu *et al.* (2002), the abyssal current can also be driven by deep water formation, the so-called source-driven current (Kawase and Straub 1991). However, this contribution seems to be smaller than that generated by the wind. Most of all, there is less and less deep water formation in the East Sea (Gamo *et al.* 1986; Kim *et al.* 2001). Even if the deep water formation rate remains unchanged, the resulting source-driven current does not become comparable to the wind-driven current in the East Sea. For example, take a deep water formation rate of order 10^{-2} Sverdrup, at which the deep water was known to be formed in the past (c.f., Kang *et al.* 2003). Assume that this happens during the period of order 10^2 days. This corresponds to deep water production of the order of 10^{11} m^3 per year. This newly formed deep water layer may spread along the periphery of the basin at a width W ($\simeq 10^2$ km) and a length L ($\simeq 10^3$ km), creating an interface elevation, say Δh, of the order of 1 m. From the geostrophic relationship, the resulting along-slope current V ($=g'\Delta h/f_0 W$) is found to be of the order 10^{-3} m/sec.

It should be mentioned that this model does not explain how the abyssal circulation is created. It addresses only the steady state problem and, hence, cannot explain the observed seasonal or transitional variations (Takemutsu *et al.* 1999; Senjyu *et al.* 2002). In future studies, the roles played by these time-varying components should be clarified. In this model, as well as in Rhines and Young (1982), the existing abyssal circulation is mostly along the closed geostrophic contour, along-slope in this model. The inertia of the along-slope component, called free mode, is so large that it is hardly changed by wind or frictional forcing which creates the cross-slope component of the current, called the forced mode. Hence, in the context of this model, the steady abyssal circulation, assumed to be planetary geostrophic, is not affected much by annually varying wind forcing unless other oscillatory currents are superimposed. Over all, this model is just one of many possible candidate mechanisms concerning abyssal circulation in the East Sea, such as the neptune effect or baroclinic instability suggested in the previous numerical experiment studies. More elaborated observations or numerical experiments are needed to further clarify the formation mechanism of the abyssal current in the East Sea.

Acknowledgements

This work was supported by INHA UNIVERSITY Research Grant (INHA-31626).

References

Chang, K.I., N.G. Hogg, M.S. Suk, S.K. Byun, and K. Kim. 2002. Mean flow and variability in the southwestern East Sea. *Deep-Sea Res. I*, **49**, 2261-2279.

Gamo, T., Y. Nozaki, H. Sakai, T. Nakai, and H. Tsubota. 1986. Spacial and temporal variations of water characteristics in the Japan Sea bottom layer. *J. Mar. Res.*, **44**, 781-793.

Hendershott, M. 1989. The ventilated thermocline in quasigeostrophic approximation. *J. Mar. Res.*, **47**, 33-53.

Hogan, P. and H. Hulbert. 2000. Impact of upper ocean- topographical coupling and isopycnal outcropping in Japan/East Sea models with $1/8_0$ to $1/64_0$ resolution. *J. Phys. Oceanogr.*, **30**, 2535-2561.

Holloway, G., T. Sou, and M. Eby. 1995. Dynamics of circulation of the Japan Sea. *J. Mar. Res.*, **53**, 539-569.

Isobe, A. and Y. Isoda. 1997. Circulation in the Japan Basin, the northern part of the Japan Sea. *J. Oceanogr.*, **53**, 37-381.

Kang, D.-J., S. Park, Y.-G. Kim, K. Kim, and K.-R. Kim. 2003. A moving-boundary box model (MBBM) for oceans in change: An application to the East/Japan. *Geophys. Res. Lett.*, **30**(6), 1299, doi:10.1029/2002GL016486.

Kawabe, M. 1982. Branching of the Tsushima Current in the Japan Sea. II. Numercial experiment. *J. Oceanogr.*, **38**, 183-192.

Kawamura, H. and P. Wu. 1998. Formation mechanism of Japan Sea proper water in the flux center off Vladivostok, *J. Geophys. Res.*, **103**, 21611-21622.

Kawase, M. and D. Straub. 1991. Spin-up of source-driven circulation in an abyssal basin in presence of bottom topography. *J. Phys. Oceanogr.*, **21**, 1501-1514.

Kim, K. and J.-Y. Chung. 1984. On the salinity minimum layer and dissolved oxygen maximum layer in the East Sea(Japan Sea). p. 55-65. In: *Ocean Hydrodynamics of the Japan and East China Seas*, ed. by T. Ichiye. Elsevier, Amsterdam.

Kim, K., K.-R. Kim, D.-H. Min, Y. Volkov, J.-H. Yoon, and M. Takematsu. 2001. Warming and structural changes in the East (Japan) Sea: A clue to future changes in global oceans? *Geophys. Res. Lett.*, **28**(17), 3293-3296.

Kim, K. J. and Y. H. Seung. 1999. Formation and movement of the ESIW as modeled by MICOM. *J. Oceanogr.*, **55**, 369-382.

Luyten, J. R., J. Pedlosky, and H. Stommel. 1983. The ventilated thermocline. *J. Phys. Oceanogr.*, **13**, 292-309.

Na, J.-Y., J.-W. Seo, and S.-K. Han. 1992. Monthly-mean sea surface winds over the adjacent seas of the Korea peninsular. *J. Kor. Soc. Oceanogr.*, **27**, 1-10.

Rhines, P. B. and W. R. Young. 1982. A theory of the wind-driven circulation. I. Mid-Ocean gyres. *J. Mar. Res.*, **40**, 559-596.

Senjyu, T. and H. Sudo. 1994. The upper portion of the Japan Sea Proper Water: Its source and circulation as deduced from isopycnal analysis. *J. Oceanogr.*, **50**, 663-690.

Senjyu, T., T. Aramaki, S. Otosaka, O. Togawa, M. Danchenkov, E. Karasev, and Y. Volkov. 2002. Renewal of the bottom water after the winter 2000-2001 may spin-up the thermohaline circulation in the Japan Sea. *Geophys. Res. Lett.*, **29**(7), 1149, doi: 10.1029/2001GL014093.

Seung, Y. H. 1992. A simple model for separation of East Korean Warm Current and formation of North Korean Cold Current. *J. Kor. Soc. Oceanogr.*, **27**, 189-196.

Seung, Y. H. 1997. Application of ventilation theory to the East Sea. *J. Kor. Soc. Oceanogr.*, **32**, 8-16.

Seung, Y. H. and J. H. Yoon. 1995. Some features of winter convection in the Japan Sea. *J. Oceanogr.*, **51**, 61-73

Takematsu, M., Z. Nagano, A. G. Ostrovskii, K. Kim, and Y. Volkov. 1999. Direct measurements of deep currents in the northern Japan Sea. *J. Oceanogr.*, **55**, 207-216.

Yoon, J. H. 1982a. Numerical experiment on the circulation in the Japan Sea. I. Formation of the East Korean warm current. *J. Oceanogr.*, **38**, 43-51.

Yoon, J. H. 1982b. Numerical experiment on the circulation in the Japan Sea. III. Mechanism of the nearshore branch of the Tsushima Current. *J. Oceanogr.*, **38**, 125-130.

Yoon, J. H. and H. Kawamura. 2002. The formation and circulation of the intermediate water in the Japan Sea. *J. Oceanor.*, **58**, 197-211.